SOME ASPECTS OF 704 MHz SUPERCONDUCTING RF CAVITIES*

R. Calaga
Brookhaven National Lab, Upton, NY, U.S.A.

Abstract

Recent developments in 704 MHz superconducting RF have prompted modifications of the cavity design geared towards high average current with high accelerating gradient structures. Some aspects of improvement of accelerating gradient and efficient extraction of higher order mode power in this frequency range is discussed.

INTRODUCTION

Recently superconducting RF (SRF) technology in the 704 MHz frequency range is increasingly popular for high average current and high intensity electron and proton linacs. The need for high duty factor (in some cases CW beams) make it favorable for linac technology with sub-giga Hertz frequencies both for overall accelerating efficiency and handling of higher order modes (HOM). Detailed studies from CW electron linacs and high intensity proton linacs have converged to the specific 700 MHz frequency [1, 2, 3]. Additionally, the number of cells per structure which is a typically a trade off between accelerating gradient and HOM performance has realized into a generic five-cell structure. Three future machines planned to work in the 700 MHz frequency range are listed in Table 1.

Table 1: Some parameters for three future accelerators anticipated to utilize 704 MHz superconducting elliptical cavities for the high β section of the linac

Parameter	eRHIC	SPL	ESS-S
Inj energy [MeV]	5	180	200
Max energy [MeV]	3-10	4-5	2.5
Beam current [mA]	50	20-40	
Pulse Length [ms]	-	0.4-1.9	1.5-2.0
Repetition rate [Hz]	CW	2-50	20
Peak Power [MW]	0.05	1.0	1.0
Cav/Cryomodule	6	8	8
Duty Factor	CW	4%	4%
Energy recovery eff	> 99.95 %	-	-

Each accelerating structure is expected to comprise of several five-cell SRF cavities (Niobium) in a single cryomodule operating at approximately 1.8 K as shown in Fig. 1. A continuous superconducting channel using super fluid helium is desired to reduce cryogenic complexity and avoid external noise sources onto the accelerating structures. The only existing SRF cavity at this frequency is cavity designed for the electron cooling project at RHIC [1]. The design and development of this SRF module has served as a valuable test bed and a successful demonstration of the technology. The first design although adequate for single high current module, presented a few shortcomings which required modifications for long linacs.

This paper will outline some cavity optimization procedures starting from an original design developed for the electron cooling. The initial objective of the electron cooling project was to accelerate ampere class beams and which required strong HOM damping at the cost of real estate gradient. In this paper the focus is directed towards increasing the accelerating efficiency while retaining the properties of the HOM damping from the original design. The focus is therefore directed towards optimizing cavity-transition section for a long cryomodule hosting 6-8 five-cell cavities. This cryomodule will serve as a fundamental unit for the machines specified in Table 1.

GEOMETRICAL DESIGN

The original design was proposed as a solution to provide a strongly damped multi-cell structure for CW energy recovery in the high current regime [1, 2]. The approach taken to reach the original design involved

- Optimization of fundamental mode RF parameters (see Fig. 2)
- Adopt a large aperture to reduce the overall power lost into the higher order modes (HOMs) and subsequently damp them strongly
- Mechanically stiff to provide a stable design to combat lorentz forces without cavity stiffners.

As a result, a five-cell cavity with large iris aperture (17cm) effectively operating as a single mode cavity emerged. The end-group transition from 17cm to 24 cm beam pipe was adopted to allow for efficient propagation of HOMs through the beam tube. They are later intercepted in the warm region using lossy ferrites similar to the strategy adopted in B-factories with single cell cavities. The exact aperture of 24 cm for the ferrites was fixed due to the availability of ferrites modules from a Cornell design [5]. The adoption of broad-band beam pipe dampers was an important step to ensure a simple and robust design for high current operation to extract large HOM beam power (a few kW) in cryogenic environment.

The virtue of the design providing strong mechanical stiffness and the cell-to-cell coupling made the cavity less sensitive to fabrication errors. Therefore, it required less mechanical tuning to reach the desired frequency and field

* This work was partially performed under the auspices of the US Department of Energy

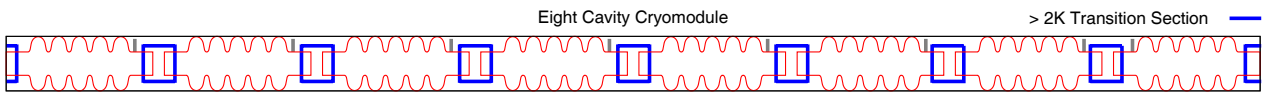

Figure 1: Schematic of an eight cavity cryomodule. The transition section between the cavities will host the couplers, tuners, HOM dampers and interconnections.

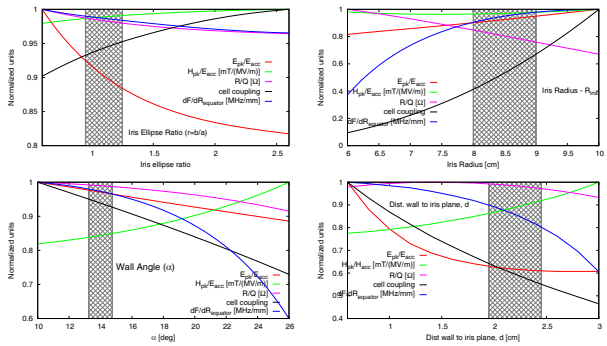

Figure 2: Parametric optimization of cavity geometry as a function relevant RF characteristics of the fundamental TM_{010} mode of the cavity [1, 2].

flatness. However, further mechanical analysis and fabrication of the five-cell cavity, it was found that the cavity stiffness was close to the yield strength of Niobium. It was determined that large tuning of the cavity by elongation or compression could potentially lead to cracks in the equator region where the cavity cells are welded. Additionally, it could result in plastic deformation of the cavity [6]. Therefore, it was deemed necessary to modify the cavity shape to reduce the stiffness while keeping the HOM characteristics similar. The RF optimization for reduced stiffness the cavity body was pursued in approximately three steps.

Fundamental Mode

Fundamental mode optimization was performed similar to the generation I cavity but for reduced cavity angle to relax the stiffness. The cavity peak fields, R/Q and cell-to-cell coupling were optimized for the mid-cell. As a result of the scan, the stiffness was approximately reduced by a factor of 2 and the peak surface magnetic field by 18% or more. This reduction in the peak magnetic field should help improve the real estate gradient proportionally. The exact reach of the gradient will however depend on the overall cavity design and appropriate treatment procedure.

HOM Frequency Scan

In addition to the fundamental mode, the mid-cell was geometry was also studied for the behavior of the first few cavity HOM modes. The HOM frequencies and their respective cut-off frequencies were scanned simultaneously as a function of the geometrical parameters. In general, the behavior of the HOM frequencies can have complicated dependencies, but the goal of this study was to identify a general trend and establish the highest frequencies for HOMs for a given aperture. This could enable in specific cases, propagation of modes which are near or slightly below the cutoff frequency of the beam pipe. Figure 3 shows the frequency dependence of various HOMs (both monopole and dipole) as a function of different geometrical parameters. It should be noted that for each change in the cavity geometry, the fundamental frequency was tuned to 704 MHz. Based on these two criteria, the mid-cell geometry is determined. In general, the optimum values for the fundamental mode overlap well with the desired values from the HOM frequency scans.

End Cell Tuning

The cavity end group (end cell and a short beam pipe section) is typically constructed from the same description of the cavity mid cell and tuned for the resonant frequency using either the equator height and/or the wall angle (α) of the end cell (for example, BNL I design). This frequency tuning sometimes results in field enhancement in the end cell which may ultimately prove to be the limiting factor the maximum cavity gradient. A trivial method is to reduce the peak fields in the end cell is to reduce the beam pipe aperture, but this is highly undesirable from field sensitivity and HOM point view. Only the cavity wall angle and iris region were optimized for minimum field enhancement for the end cell which is shown in Fig. 4. The equator ellipse is not modified to have the least impact from Lorentz force detuning. The end cell parameters with better peak magnetic field is listed in Table 2. For a comparison, the peak magnetic field is 1.6% smaller in the cavity structure with modified end cell compared to a structure using the same geometrical parameters as the mid-cell. It should also be noted that no mechanical considerations are taken into effect here and may impact the proposal to reduce the cavity wall angle.

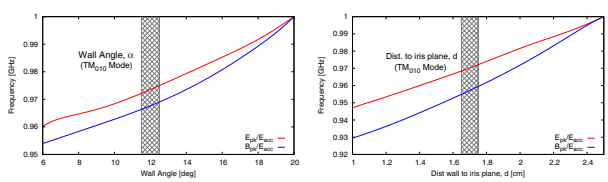

Figure 4: Field enhancement scan for the TM_{010} mode using the cavity wall angle and iris region of the end group.

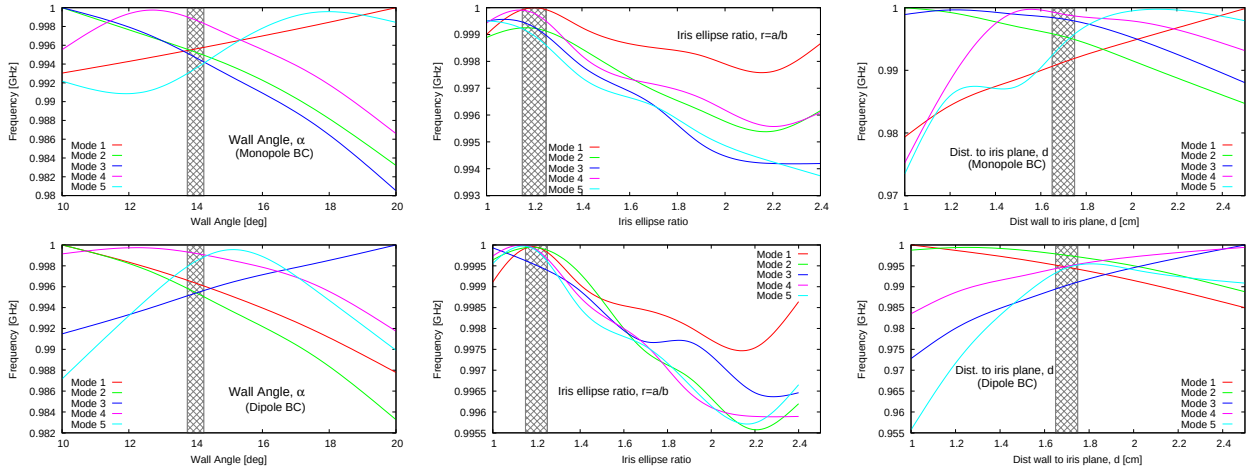

Figure 3: The frequency evolution of the first five monopole modes (top) and first five dipole modes (bottom) as function of geometrical parameters.

HOM CONSIDERATIONS

There are also important criteria for HOM damping in SRF structures which will confine the aperture to an optimum values. As the number of cells grow in multi-cell cavities, the cell-to-cell coupling becomes of great significance to avoid trapped modes and perform efficient tuning of individual modes. In addition, the weaker coupling can impact the field sensitivity and thereby play a significant role in field flatness and mode damping due to cavity imperfections. Cell-to-cell coupling and difference in the mid-cell and the end-cell as suggested in Ref. [1, 2, 7] are evaluated.

Mid-cell

The iris aperture of the mid and the end-cells are varied with the cavity parameters fixed to previous optimized values (see Table 2). The cell-to-cell coupling is defined as

$$\frac{1}{\kappa} = \frac{1}{2}\frac{f_M - f_E}{f_M + f_E} \qquad (1)$$

where f_M and f_E correspond to frequencies calculated with boundary conditions imposed on cavity ends. Figure 5 shows the cell-to-cell coupling for first five monopole and dipole modes of the cavity mid-cell and end-cell as a function of aperture. The aperture radius of 8.5 cm is reasonably suited for both monopole and dipole modes to have sufficient cell-to-cell coupling without compromising the fundamental performance. It is also evident from this scan that a decrease of the aperture to 7.5 cm has relatively small effect on the HOMs while minimizing the relative frequency shift of fundamental mode to mechanical imperfections.

End-cell, Frequency Domain

The addition of the end group with beam pipes require the tuning of the mainly by the end-cell to rematch to the

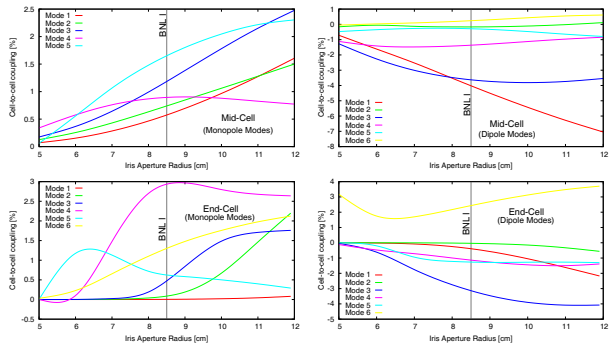

Figure 5: Top: Aperture scan to calculate cell-to-cell coupling for first few modes in the mid cell with monopole dipole modes. Bottom: Aperture scan to calculate cell-to-cell coupling for six modes in the end group with monopole and dipole modes.

resonant frequency. Due to the retuning of the fundamental mode, it is possible that the mid-cell and end-cell resonate differently for different HOM passbands [1, 2]. If the frequency difference becomes vastly different, it becomes difficult to avoid trapped modes in the center of the cavity without easy means to damp them. The reduction of the frequency difference in the BNL II design is studied only as a function of the iris aperture as the other parameters are already fixed from previous scans. From Fig. 6, the reduction of the frequency difference between mid-cell and end-cell calls for a reduction in the aperture. An aperture radius of approximately 7.5 cm can reduce the frequency difference for most modes with some marginal compromise on the cell-to-cell coupling.

End-cell, Time Domain

Time domain simulations were also carried to estimate the longitudinal and transverse impedances as a function of aperture to understand the coupling impedance charac-

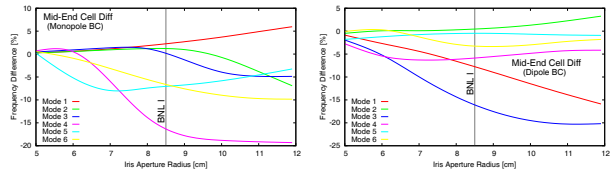

Figure 6: Aperture scan to estimate the influence on the frequency difference between the mid and end cells for the first few modes with monopole and dipole modes.

teristics. The impedance is obtained from wake potentials calculated numerically using ABCI [8] for end groups with varying radii, but always tuned to 704 MHz for a fundamental mode frequency. Figure 7 shows impedance spectrum of both monopole and dipole modes as a function of iris aperture. The impedance is calculated from a wake of 100 m corresponding to a medium range wake. It should be noted that the exact impedance for modes below the cut-off of the beam pipe may not be accurate due to artificial wake truncation. However, the trend of the impedance spectra is clearly visible.

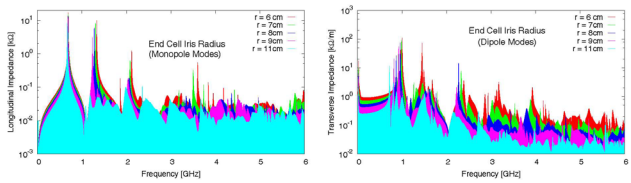

Figure 7: Aperture scan to estimate the impedance influence on the frequency difference between the mid and end cells for the first few modes with monopole and dipole modes.

Although there is no single optimum aperture, a minimum aperture suited for HOM damping is preferred to maintain the best acceleration efficiency. Based on the frequency and time domain results, the minimum aperture can be confined to 7.5cm which is used as a baseline for further calculation in the multi-cell models. An alternative 8.5 cm iris is also used for comparison when required.

FINAL DESIGN

It should be noted once again that the parametric scans are non-orthogonal and there exists no unique solution that satisfy requirements for all modes in the cavity. However, the above optimization relies on general trends observed from these scans to find a well chosen region which is not always obvious from complex structures. A set of parameters are proposed for a "semi-optimum" design for the improved BNL II design listed in Table 2. The corresponding middle and end cells are depicted in Fig. 8 for the two designs.

Table 2: Cavity geometrical parameters

Parameter	BNL I {Mid, End}	BNL II {Mid, End}
Frequency [MHz]	703.75	703.75
Iris Radius, R_{iris} [cm]	8.5	8.5
Wall Angle, α [deg]	25	{14,12}
Equatorial Ellipse, $R = \frac{B}{A}$	1.0	1.0
Iris Ellipse, $r = \frac{b}{a}$	1.1	1.2
Cav wall-iris plane, d [cm]	2.5	{1.7,1.2}
$\frac{1}{2}$ Length, $L = \frac{\lambda\beta}{4}[cm]$	10.65	10.65
Eq. Radius [cm]	20.9	{19.7,19.4}
Cavity Beta, $\beta = \frac{v}{c}$	1.0	1.0

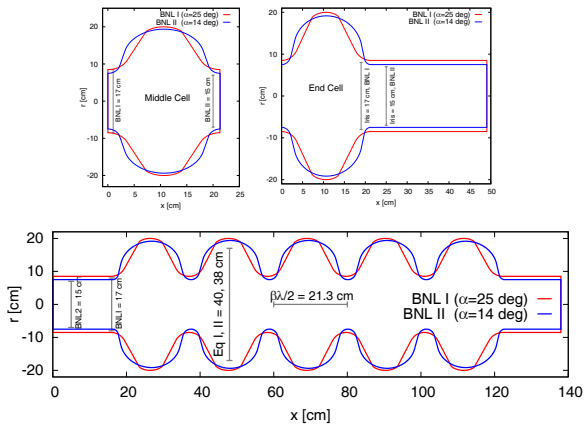

Figure 8: Top: Mid and end cell geometries for 703.75 MHz superconducting cavity. Bottom: Almost final five-cell geometry of the BNL II design compared to the original BNL I design. The two curves represent BNL I (original) and BNL II modified designs.

TRANSITION SECTION

Unlike the design goal of BNL I cavity which was aimed at minimizing trapped modes and accomplish strong damping, it is desirable to minimize the length of the transition section between subsequent cavities. It is envisioned that the typical 704 MHz cryomodule will consist of 6-8 cavities and the cyomodules will stacked in a long linac configuration at 2K with minimal thermal transitions. This

Table 3: RF parameters for final mid and end cells for the BNL II design compared to the original BNL I design

Parameter	BNL I	BNL II
Frequency [MHz]	703.75	704
Number of cells	5	5
E_p/E_a	1.97	2.16
H_p/E_a [mT/MV/m]	5.78	4.45
R/Q [Ω]	404	497
dF/dR [MHz/mm]	4.18	3.83
Cell-cell coupling	3%	2.99%

eliminates the possibility of using 300 K ferrite absorbers on the beam pipes which required at the very high current and CW regime. Therefore, alternate solutions are considered to design a short transition section (≤0.5-0.6 m) while maintaining two important criteria

- Maintain strong damping as in BNL I and use the beam pipe to propagate the HOMs to the dedicated couplers located within the transition section.
- Minimize cross talk for the operating mode between the cavities.

Therefore, three different options are being considered for the most effective interconnection as shown as in Fig. 9. The exact diameter of the transition from end-cell to the beam pipe will be the outcome of future studies to improve the propagation of HOMs into the transition section. Based on the final aperture of the beam pipe, the transition step will be optimized to minimize cross talk. The step will additionally provide an enhancement of the HOM fields so increase the coupling to the HOM probes located across the step.

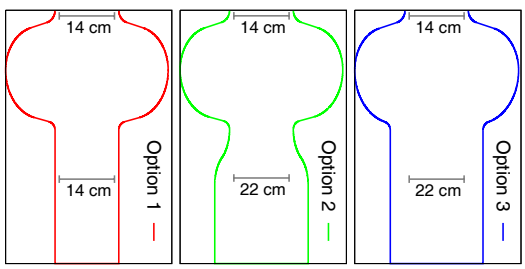

Figure 9: Three different transition sections concepts for the interconnection between two cavities.

High current CW beams may require stronger damping of potentially semi-trapped dipole modes (for example, TM_{110}) to suppress transverse instabilities. Therefore, a special four ridged (or three ridged) structure is proposed for the beam pipe to enhance the propagation of dipole and other HOMs to the probes located across the transition step. A conceptual schematic is shown in Fig. 10.

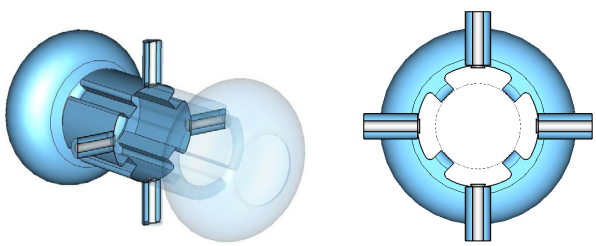

Figure 10: A ridged beam pipe concept to suppress the fundamental mode propagation into the beam pipe while retaining the propagation of dipole and HOMs.

A unique feature of the ridge allows selective suppression of the fundamental mode, first used in the B-factory at Cornell in the form of flutes [9]. Figure 11 shows the suppression of the fundamental mode propagation as a function of beam pipe length. Two different transition sections (8.5 cm and 8.5-to-12 cm) are compared to the ridge structure. The exact suppression will depend on the final ridge dimensions.

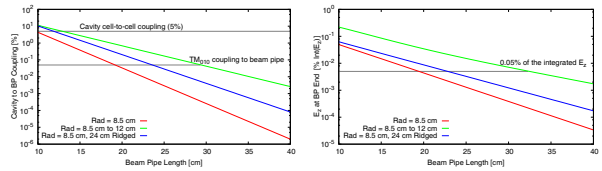

Figure 11: Top: Cavity to beam pipe coupling as a function of beam pipe length for three different beam pipe configurations (smooth, enlarged, ridged). Bottom: E_z on axis at the beam pipe edge normalized to the field gradient as a function of beam pipe length.

CONCLUSION

A detailed design evaluation of the original 703.75 MHz cavity developed for electron-cooling led to modifications suited for future high energy linacs operating near 704 MHz. The modifications were incorporated and the cavity was further optimized for both fundamental mode and HOMs. Further studies are needed to evaluate the exact cavity geometry together with the interconnection for efficient extraction of HOMs and reduced losses from the fundamental mode.

ACKNOWLEDGMENTS

The author would like to thank I. Ben-Zvi, J .Burill, F. Gerigk, J .Sekutowicz, G. McIntyre for valuable discussions.

REFERENCES

[1] R. Calaga, Ampere class SRF cavities, Ph.D. Thesis, 2006.
[2] R. Calaga et al., High current energy-recovery superconducting linacs, *to be submitted to PRST-AB*.
[3] F. Gerigk et al., Choice of frequency, gradient and temperature for a SPL, CERN-AB-2008-064., 2008.
[4] I. Ben-Zvi et al., Electron Cooling of RHIC, PAC05, Knoxville, 2005.
[5] D. Moffat et al., PAC93, IEEE Publishing, Piscataway, New Jersey, 1993.
[6] D. Holmes, *private communication*.
[7] J. Sekutowicz, New Geometries Overview, ANL, September 22, 2004.
[8] Y. H. Chin, ABCI Version 8.7, CERN, Geneva.
[9] H.Padamsee et al., PAC91, San Francisco.